

HYDRODYNAMIC ANALYSIS OF STATIC WATER IMPACT ON

WEDGE-SHAPED HULL WATERTIGHT TEST SPECIMEN THROUGH

NUMERICAL ANALYSIS

Muwen Niu¹, Feng Sun², Chenxi Du³, Heyuan Huang^{1,4,*}

¹Northwestern Polytechnical University, Xi'an, China

²Xi'an Modern Control Technology Research Institute, Xi'an, China

³AVIC XAC COMMERCIAL AIRCRAFT CO., LTD., Xi'an, China

⁴Aircraft Strength Reserch Institute of China, Xi'an, China

Abstract

Large amphibious aircraft, primarily tasked with sea rescue and firefighting missions, and their wedge-shaped hull is mainly composed of metal and composite materials. Unlike the energy state during land landing, which has been extensively studied, amphibious aircraft landing on water will face more complex situations and severe overloading, this overload is a key factor in the strength design of these aircraft structures, and the potential damage to the structure cannot be ignored. Therefore, analyzing the static water impact of amphibious aircraft is essential. A review of the CCAR-25-R4 'Airworthiness Standard for Transport Aircraft' [4] reveals that the hull is the primary load-bearing structures during water landings.

As the first part of this study, this paper aims to study the bottom pressure situation of amphibious aircraft during water landing. Using computational fluid dynamics software FLUENT, numerical calculations were conducted on the landing response of a wedge-shaped hull watertight test specimen in still water, and the pressure time history of multiple measurement points during the process was provided.

Using ICEM software to partition the flow field mesh during the water landing process of the test specimen, the entire fluid domain is divided into unstructured mesh and consists of two parts: the accompanying mesh area and the dynamic mesh area. The shape of the surrounding mesh changes significantly during the falling process of the test specimen, and the flow field mesh needs to be adjusted according to the movement of the rigid boundary of the test specimen, so the dynamic mesh method is used for processing.

FLUENT software is used for water response calculation, and the Fluid Volume Function (VOF) method is adopted for processing. This method tracks the interface between phases by solving the continuous equation of the volume fraction of each phase fluid. Set up pressure monitoring points at the bottom of the test specimen to obtain the changes in bottom pressure of the test specimen under different weights and landing speeds, providing reference for the airworthiness verification of this type of amphibious aircraft.

Keywords: amphibious aircraft; water landing test; fluid-structure interaction; wedge-shaped hull

1. Calculation Method

In recent years, many scholars have studied the strength characteristics of metal and composite materials [1,2]. Unlike the energy state during land landing, which has been extensively studied [3], amphibious aircraft landing on water will face more complex situations and severe overloading, this overload is a key factor in the strength design of these aircraft structures, and the potential damage to the structure cannot be ignored. With the development of numerical simulation technology, the application of numerical methods to solve CFD models in engineering is becoming increasingly widespread. At present, some commonly used computational fluid dynamics analysis software such as FLUENT, CFX, etc. can simulate many common problems such as multiphase flow, heat transfer, etc., and the solution accuracy has been greatly improved. This paper applies CFD software FLUENT system to numerically simulate the landing pressure history of two-phase mixed fluids under different weight and speed conditions for wedge-shaped ship hull configurations. The following provides a brief overview of the numerical calculation methods for two-phase flow response using FLUENT software.

1.1 Finite Volume Method

The FLUENT system is based on an unstructured Euler grid format and utilizes finite volume discretization method to perform numerical calculations [5]. The basic idea is to divide the calculation area into grids and have a non-repeating control volume around each grid point; Integrate the differential equation (control equation) to be solved for each control volume to obtain a set of discrete equations. The unknown variables are the dependent variables on the grid points. In order to obtain the integral of the control volume, it is necessary to assume the variation law of the dependent variable between grids. From the perspective of the selection method of the integration region, the finite volume method belongs to the subdomain method of the weighted residual method. From the perspective of the approximation method without known solutions, the finite volume method belongs to the discrete method using local approximation. In short, the subdomain method plus discretization is the basic method of finite volume method.

1.2 Fluid Volume Function Method

The fluid volume function method (VOF) is used to describe and capture the free interface between the water and air phases involved in this study, and this method is used to trace the interface between phases by solving a continuous equation for the volume fraction of each phase of the fluid.

For the two-phase flow problem in this report, some units have only one fluid phase, while others belong to interface units composed of two-phase fluids. The properties of this unit are determined by the properties of the two-phase fluid and their respective volume fractions in the unit.

In this paper, the use of VOF method can effectively simulate the effects of air and water on watertight test specimens.

1.3 Moving Grid Method

In the calculations in this study, the watertight test specimen landing is a rigid movement of the boundary, which causes the shape of the fluid domain to change with time, so the mesh of the fluid domain needs to be adjusted with the movement of the boundary [6]. In this study, a moving mesh model is used for mesh adjustment.

2. Algorithm Validation

To verify the correctness of the numerical calculation method and software parameter settings, a simple two-dimensional cylindrical water contact response was calculated before calculating the static water contact response of the watertight test specimen, and compared with the experimental data in reference [7].

2.1 Numerical Simulation of Two-dimensional Cylinder Submerged in Water

Use ICEM software to establish a computational model and conduct numerical research on two-dimensional cylindrical water landing.

The radius R_1 of the cylinder is 0.1m, and the pressure change at point P with a central angle of 0° is monitored during the calculation process. The model weight is 62.5kg. The calculation domain is 2.5m high and 2.0m wide. Initially, the center of the cylinder is 1.0m away from the top of the calculation domain, as shown in Figure 1.

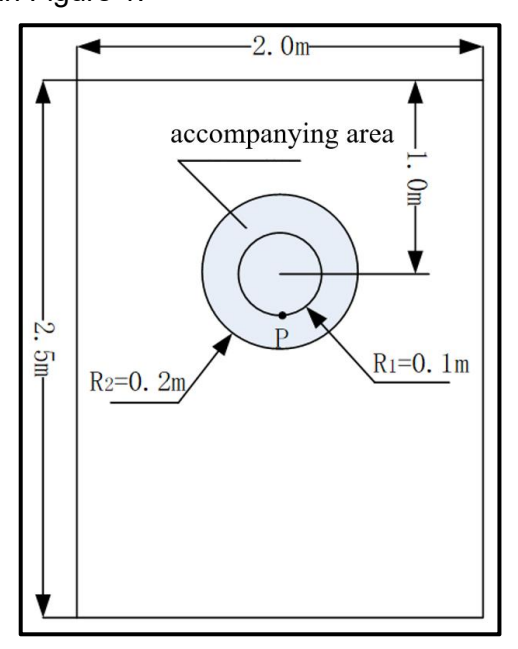


Figure 1 – Schematic diagram of cylindrical water landing calculation domain

The initial velocity is 2m/s, and the cylinder is 0.03m away from the water surface at the initial moment. There is an accompanying area with a radius of R_2 =0.2m around the cylinder, which moves along with the cylinder to ensure the quality of the mesh around the cylinder during the calculation process. The other areas are deformed mesh areas, which are reconstructed using elastic smoothing and mesh reconstruction methods. All regions are divided into triangular unstructured grids, with approximately 23500 grids. Figure 2 shows the initial moment of numerical calculation in FLUENT, with blue representing the water phase and red representing the air phase.

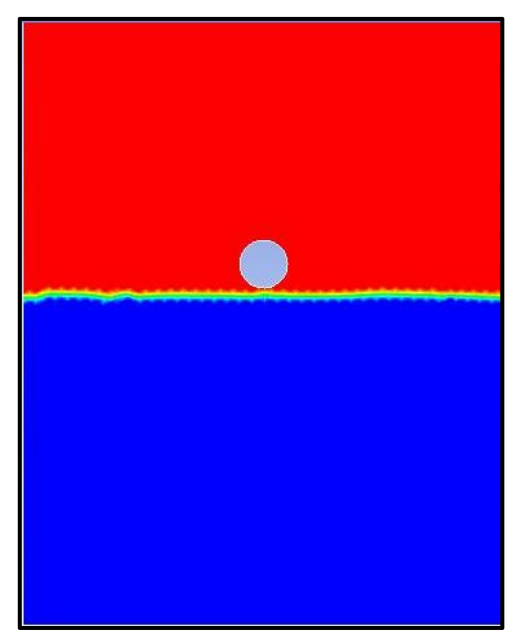
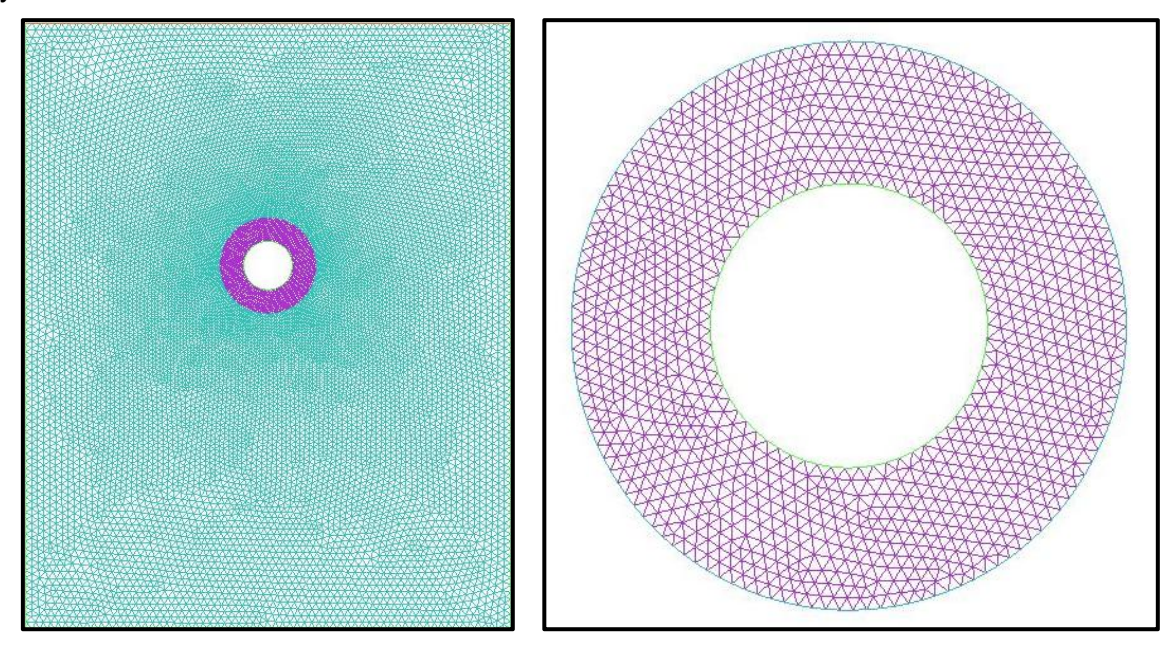


Figure 2 – Initial time diagram of cylindrical water landing simulation

Figure 3 shows the grid of the entire computational domain and the accompanying grid area around the cylinder.



(a) Overall grid (b) Grid of accompanying area Figure 3 – Cylindrical water landing grid situation

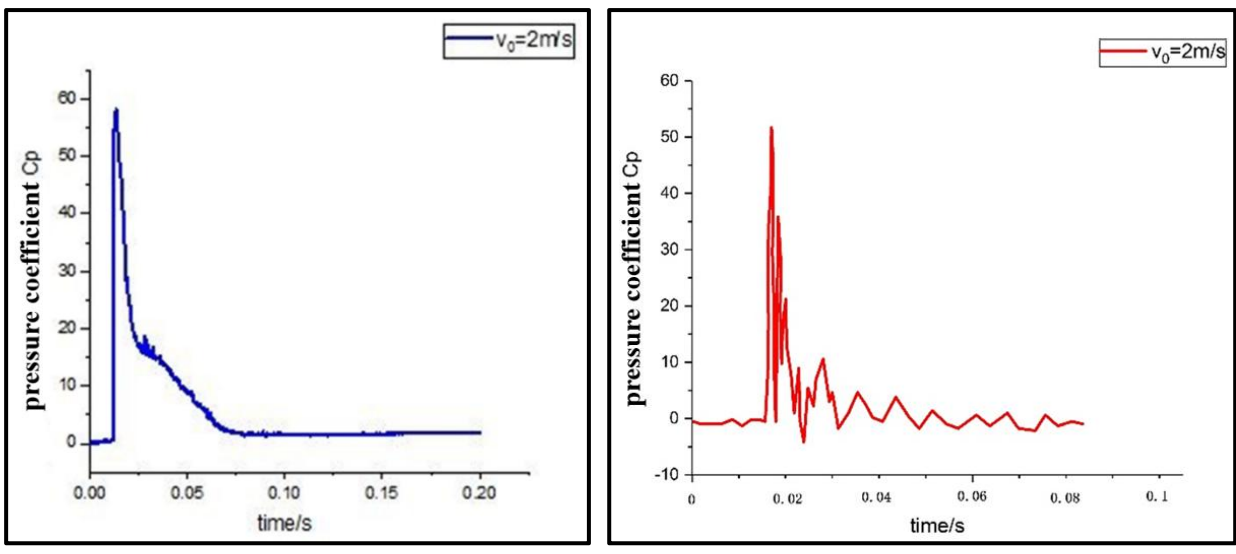
2.2 Comparison Between Numerical Calculation Results and Experimental Results The formula for calculating the pressure coefficient C_p is:

$$C_p = (p - p_{ref})/(0.5\rho v^2)$$
 (1)

Among them: p is static pressure; P_{ref} is the reference pressure, which is taken as 0 in the calculation of this paper.

The pressure coefficient curve of numerical simulation over time and the experimental results in

reference [4] are shown in Figure 4.



(a) Numerical simulation result (b) Experimental result

Figure 4 – Comparison of experimental and numerical simulation results

From the above figure, it can be seen that the cylinder first accelerates and falls under the action of gravity. After about 0.015 seconds, it collides with the water surface, generating a strong impact load on the bottom monitoring point, causing it to reach its peak water pressure. Subsequently, due to the damping effect of water, the cylinder velocity decreases and the load gradually stabilizes.

By comparison, the peak pressure coefficient calculated numerically is basically consistent with the experimental results.

3. Structural Model Parameters

The watertight test specimen calculated numerically in this study is a geometric seal of a symmetrical wedge-shaped bottom, as shown in Figure 5 below.

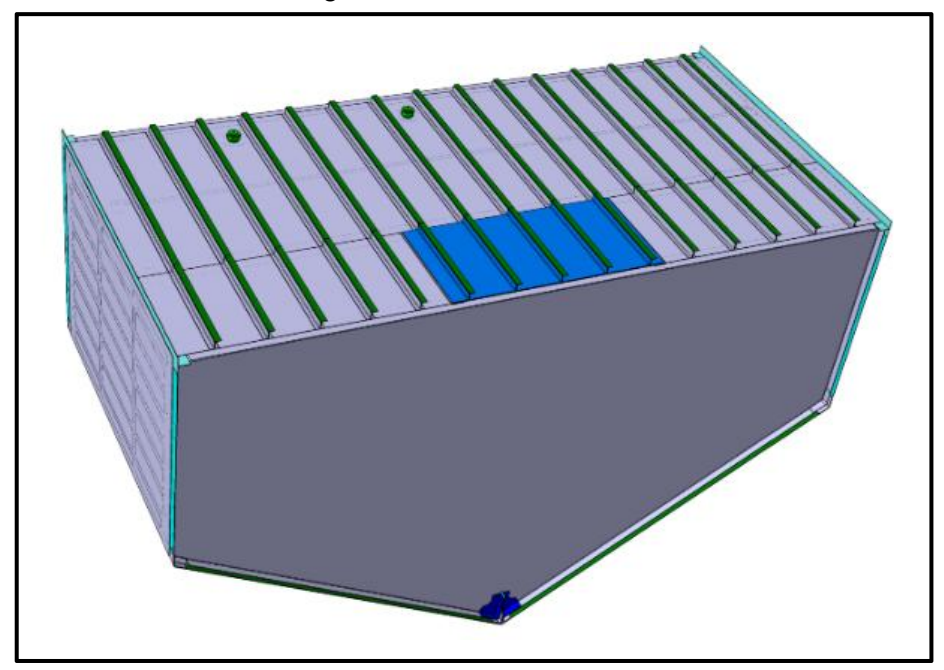
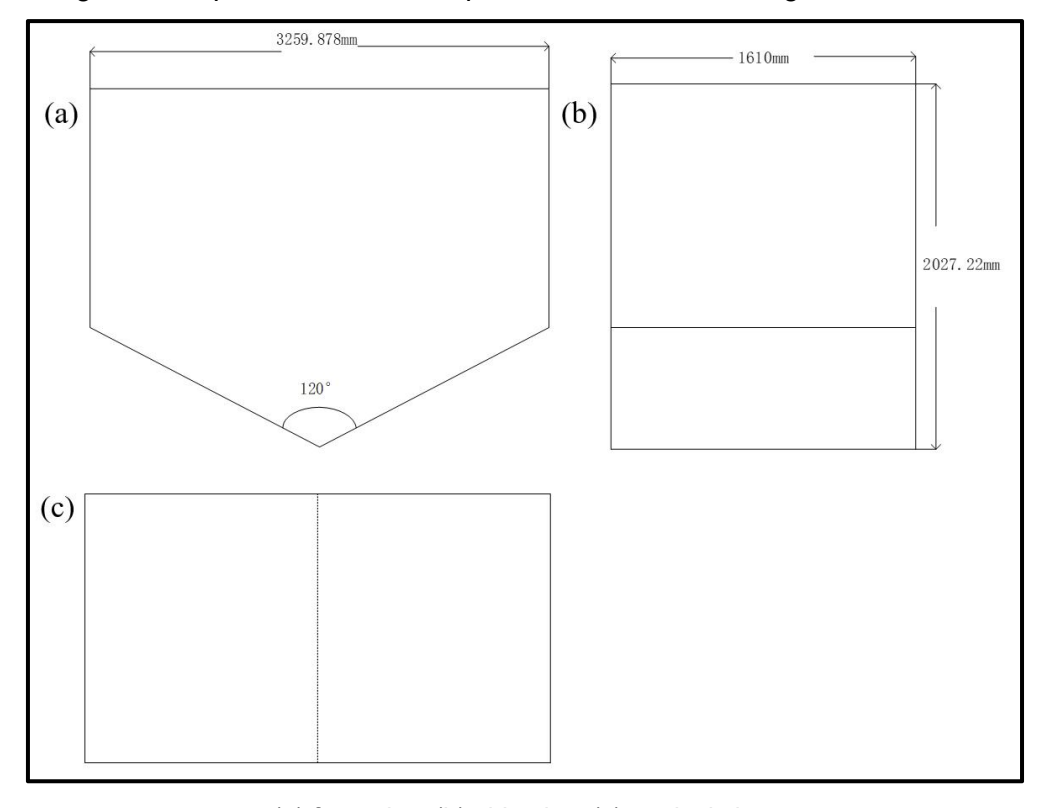


Figure 5 – Schematic diagram of watertight test specimen

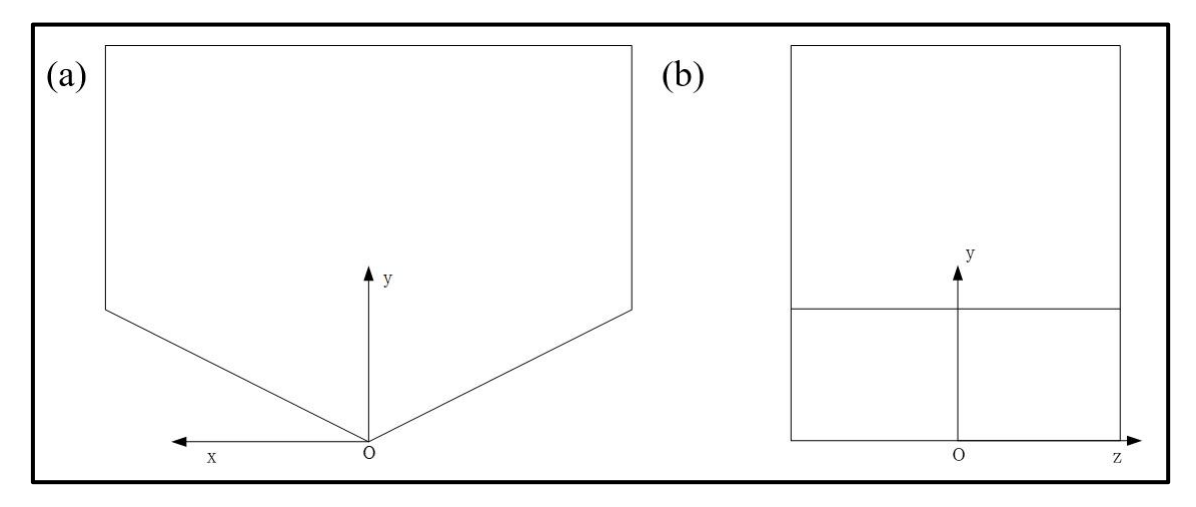
The geometric top wall panel is reinforced, with smooth wall panels on the front and rear planes, as well as on the left and right sides. The wedge-shaped sloping surfaces are reinforced wall panels. The three views and geometric parameters of the specimen are shown in Figure 6.



(a) front view (b) side view (c) vertical view

Figure 6 – Three views of watertight test specimen

Establish a coordinate system as shown in Figure 7, with the midpoint of the wedge-shaped pointed bottom of the test specimen as the origin, length as the x-axis, height as the y-axis, and width as the z-axis. Due to the inability to determine the mass distribution of the watertight test specimen, the center of gravity was taken at (0,1200,0) during numerical calculations, and the moment of inertia of the test specimen was taken as $I_x=129 \text{kg} \cdot \text{m}^2$, $I_y=111 \text{kg} \cdot \text{m}^2$, $I_z=129 \text{kg} \cdot \text{m}^2$.



(a) Coordinate system front view (b) Coordinate system side viewFigure 7 – Coordinate system setting

4. Static Water Response

4.1 Computational Models and Meshing

Use ICEM software to establish structural geometric models and calculate flow fields, and partition grids. The distance between the left and right ends of the calculation domain and the test specimen is 10 times the length of the test specimen, the front and rear ends are 5 times the length of the test specimen, and the upper and lower ends are also 5 times the length of the test specimen, as shown in Figure 8.

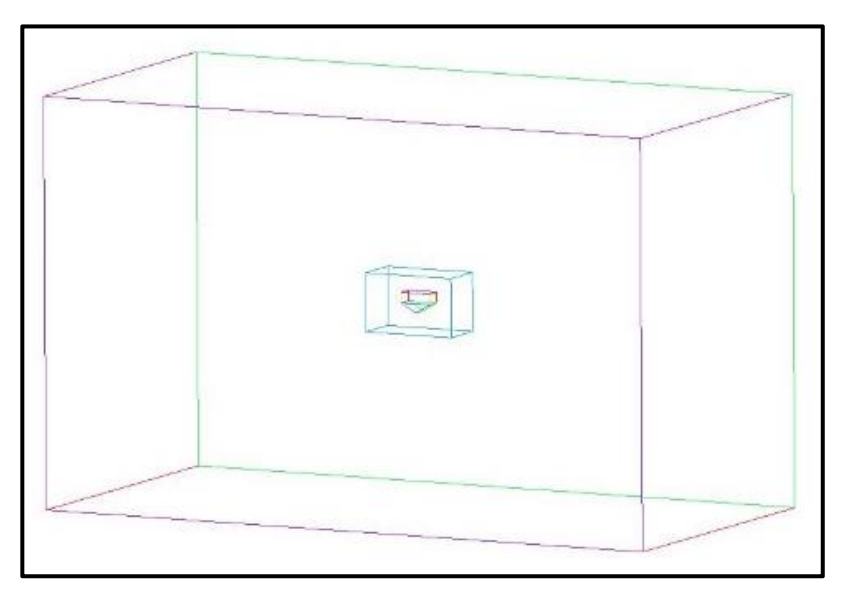
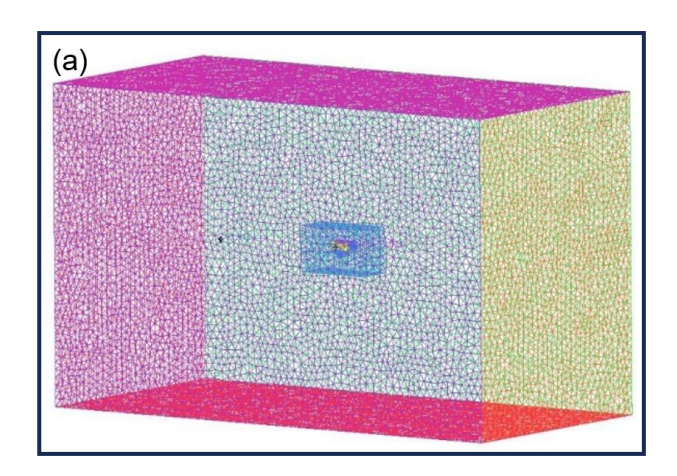
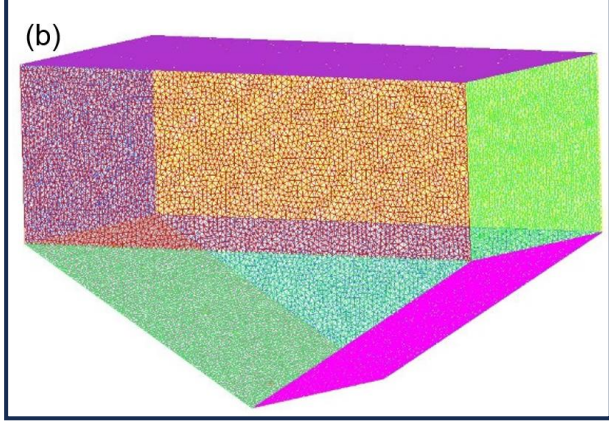


Figure 8 – Schematic diagram of calculation area

Unstructured grid partitioning is used within the computational domain, including both air and water parts. To ensure the quality of the mesh around the test specimen, the mesh division around the test specimen is relatively dense, and an accompanying mesh area is added around it to wrap the test specimen. The mesh in this area moves together with the test specimen during calculation and does not undergo reconstruction. Figure 9 shows the grid situation, with a total of 1.67 million grids.

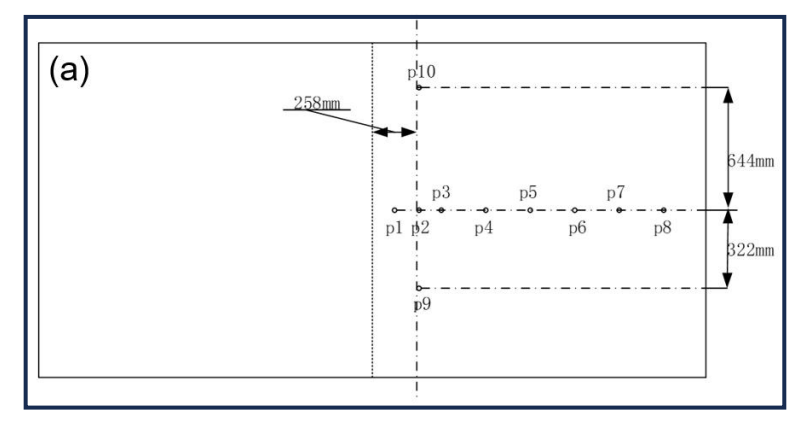


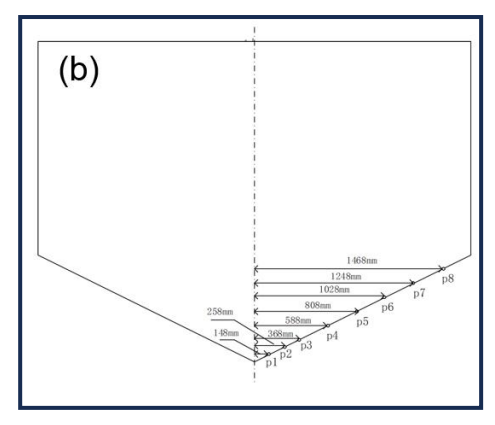


(a)Schematic diagram of the overall grid (b) Grid distribution on the surface of the specimen Figure 9 – Schematic diagram of watertight test specimen

4.2 Pressure Monitoring Point Setting

In order to monitor the pressure at the bottom of the watertight test specimen when it is wet, 10 pressure monitoring points P_1 to P_{10} are set on the right inclined plane of the wedge, as shown in Figure 10.





(a) Top view of the location of the monitoring point (b) Positive view of the location of the monitoring point

Figure 10 – Location of the pressure monitoring point

4.3 Static Water Landing Conditions

When the watertight test specimen hits the water, the influence of the weight and descent speed of the specimen on the water response is mainly considered, there are 3 specimen weights and 7 descent speeds were test, for a total of 13 different conditions, this is shown in Table 1.

Landing conditions	Weight of specimen (kg)	Descent speed (m/s)	Drop height (m)	
1	406	2	0.204	
2	406	4	0.815	
3	406	6	1.835	
4	600	2	0.204	
5	600	4	0.815	
6	600	6	1.835	
7	1200	1	0.051	
8	1200	2	0.204	
9	1200	3	0.459	
10	1200	4	0.815	
11	1200	5	1.274	
12	1200	6	1.835	
13	1200	7	2.497	

Table 1 – Watertight test specimen water condition

4.4 Calculation Results

The FLUENT computational fluid dynamics software was used to simulate the watertight test specimen's water response, and the numerical simulation results of each pressure monitoring point when the watertight test specimen landed on the water surface were given, and compared with the test results, taking the specimen's weight of 1200kg and the descent speed of 7m/s as an example, the results are as follows.

	Table 2 Companion of namendal calculations with experimental recalls										
		Monitor point pressure peaks (Kpa)									
	P_1	P_2	P_3	P_4	P_5	P_6	P ₇	P ₈	P_9	P ₁₀	
Test results	93.74	88.49	77.38	57.83	40.55	27.22	19.83	10.35	85.15	58.20	
Numerical calculations	97.90	92.71	81.41	62.64	44.03	26.59	19.79	13.17	92.28	67.17	
Deviation	4 7%	4 8%	5 2%	8 3%	8.6%	-2 3%	-0.2%	27 2%	8 3%	15.4%	

Table 2 – Comparison of numerical calculations with experimental results

Through comparative analysis, the numerical calculation results under 13 landing conditions are generally consistent with the test results, and the deviation of most of the data is about 10%, which meets the requirements of engineering deviation accuracy.

The pressure of each monitoring point under landing condition 13 (watertight test specimen weight 1200kg, descent speed 7m/s) changes with time as shown in Figure 11.

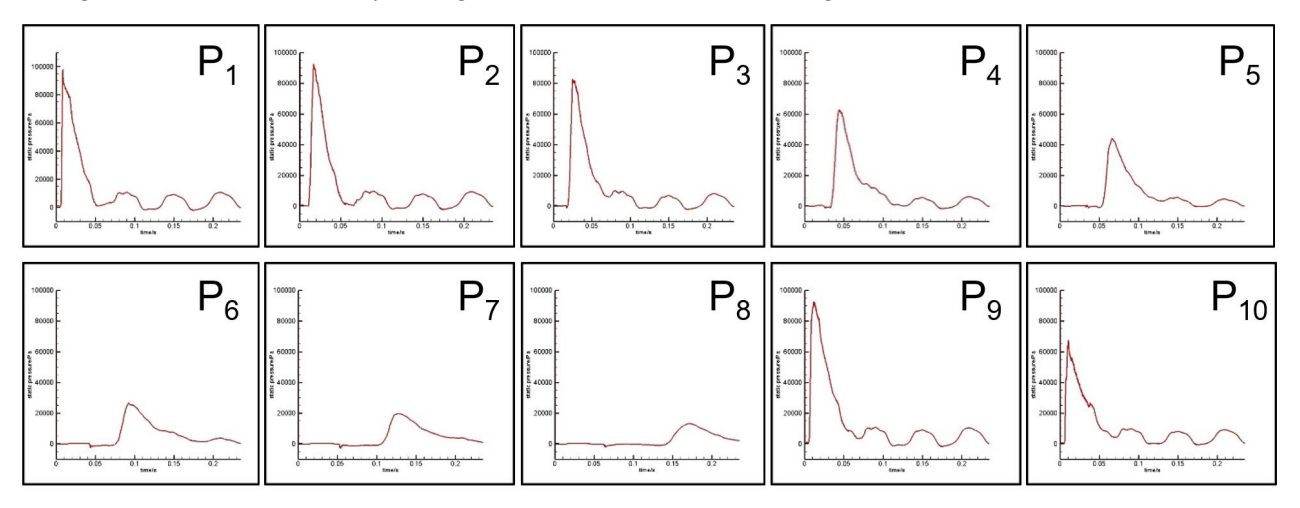


Figure 11 – P₁-P₁₀ point pressure-time curves

5. Conclusion

Through the simulation analysis of the hydrostatic response of the watertight test specimen, the following conclusions are drawn:

- (1) Under 13 landing conditions, the distribution of water pressure at all monitoring points was the same, that is, the peak pressure at P₁ was the largest, the peak pressure decreased from P₁ to P₈, and the pressure peak value at P₉ and P₁₀ was close to that of P₂.
- (2) At the same descent rate, the weight of the specimen increases from 406kg to 1200kg, and the peak water pressure at each monitoring point at the bottom of the specimen also increases. The descending speed of the specimen increases from 1 m/s to 7 m/s, and the water pressure at each monitoring point at the bottom of the specimen also increases when the weight remains the same.
- (3) When the watertight test specimen falls vertically, the water pressure at the bottom of the test specimen also increases with the increase of the descending speed and the weight of the test specimen itself, and the water impact of the descending speed is greater.

6. Contact Author Email Address

The contact author email address: huangheyuan@nwpu.edu.cn.

7. Copyright Statement

The authors confirm that they, and/or their company or organization, hold copyright on all the original material included in this paper. The authors also confirm that they have obtained permission, from the copyright holder of any third-party material included in this paper, to publish it as part of their paper. The authors confirm that they give permission, or have obtained permission from the copyright holder of this paper, for the publication and distribution of this paper as part of the ICAS proceedings or as individual off-prints from the proceedings.

References

- [1] Li G.W, Cao E.T, Jia B, Zhang X.J, Wang W.Z and Huang H.Y. Mechanical properties and failure behaviors of T1100/5405 composite T-joint under in-plane shear load coupled with initial defect and high-temperature. *Composite Structures*, Vol. 328, 2024.
- [2] Li G.W, Dong Z.C, Luo T.H and Huang H.Y. Study on the influence of shot peening strengthening before shot peen forming on 2024-T351 aluminum alloy fatigue crack growth rate. *Scientific Reports*, Vol. 13, No. 1, 2023.
- [3] Hu Y.H, Yan J.Q, Cao E.T, Yu Y.M, Tian H.M and Huang H.Y. Approach and landing energy prediction based on a long short-term memory model. *Aerospace*, Vol. 11, No. 3, pp 226, 2024.
- [4] CCAR-25-R4,25.521-25.537: Water load, Civil Aviation Administration of China.
- [5] Han Z.Z. FLUENT—Fluid Engineering Simulation Calculation Examples and Analysis. 1st edition, Beijing Institute of Technology Press, 2009.
- [6] Zhang X, Wang Y.R, et al. Research on fluid-structure interaction method based on multilayer dynamic grid technology. *Ship Engineering*, Vol. 31, No. 1, pp 64-74, 2009.
- [7] Lin M C, Shied L D. Flow visualization and pressure characteristics of a cylinder for water impact. *Applied Ocean Research*, Vol. 19, No. 2, pp 101-112, 1997.